Particle Simulation of Electrodynamic Aerobraking in a Hypersonic Rarefied Regime

Hiroshi Katsurayama* and Takashi Abe†

*Yamaguchi University, Yamaguchi 755-8611, Japan
†Japan Aerospace Exploration Agency, Kanagawa 229-8510, Japan

Abstract. To investigate the electrodynamic aerobraking in a hypersonic rarefied regime, the electromagnetic flow control on a reentry Hayabusa-shape capsule entering a pure nitrogen atmosphere is investigated using the Direct Simulation Monte Carlo method with a simple ion particle movement method like the Particle-In-Cell method. As a results, the generated electrodynamic force is found to be enough strong to use the electrodynamic aerobraking.

Keywords: Hypersonic Rarefied Flow, Reentry, Aerobraking
PACS: 52.65.Pp

INTRODUCTION

Aerobraking is a promising orbital insertion technique in planetary exploration missions because the aeroassisted spacecraft deceleration through a planetary atmosphere can save huge on-board propellant required for the deceleration using a chemical motor. In 2002, The Mars Odyssey mission [1] has successfully demonstrated the aerobraking orbital maneuvering from a Mars orbit after the orbital insertion using a chemical motor. In the aerobraking mission, on-board flat panels without any Thermal Protection System (TPS) was expanded to control increasing aerodynamic drag. However, a structure without any TPS is not applicable to a direct aerobraking orbital insertion (that is, aerocapture) because a spacecraft are exposed to severe convective and radiative heating. Although ballute technology [2] is proposed to control aerodynamic drag at a high altitude in which heat load is small because of rarefied atmosphere, the TPS problem has been still one of obstacles to realize the aerocapture technology.

An alternative to existing aerobraking technology can be achieved by actively controlling aerodynamic drag through an electromagnetic force which is generated by applying a magnetic filed to a partially ionized flow behind a bow shock around a spacecraft [3, 4, 5]. Figure 1 shows a schematic view of electrodynamic aerobraking. A magnet embedded in a blunt body forms a dipolar-like magnetic field $\boldsymbol{B}$ around the body, and a circumferential current J_θ is induced according to Ohm's law through the interaction between $\boldsymbol{B}$ and the weakly ionized flow $\boldsymbol{v}$ behind a bow shock. The electromagnetic effect generates the Lorentz force $\boldsymbol{J}\times\boldsymbol{B}$ against the flow direction, and the shock standoff distance is enlarged: the effect reduces aerodynamic heating and increases aerodynamic drag because the effective radius of curvature of the body increases from the viewpoint of the bow shock (in practice, $\boldsymbol{J}\times\boldsymbol{B}$ acting on the fluid exerts a reaction force on the magnet [5]). Moreover, electrodynamic aerobraking is more advantaged than aerodynamic aerobraking with a structure because drag is easily controllable by changing the magnetic strength.

To make the electromagnetic flow control effective, the magnetic interaction parameter [6] Q requires a condition by which

$$Q = \left(\sigma B^2 L\right) / \left(\rho_\infty v_\infty\right) \gtrsim 1 \ , \tag{1}$$

where σ, $\rho_\infty v_\infty$, and L respectively represent electric conductivity, the momentum of the flow, and the characteristic length of the body. To apply this flow control to the reentry TPS, many researchers studied this topic in the 1950–1970s theoretically [3, 4, 5] and experimentally [7, 8, 9], and these early experiments have shown the luminous shock layer enlargement [7], heat flux reduction [8], and drag increase [9] through the electromagnetic effect. However the electrodynamic TPS has not been realized because the applied field required for $Q>1$ is too strong for actual applications. Nevertheless, recent technological advancements of superconductive materials has made it possible to develop a magnet with the necessary strength: an on-board magnet or coil can be applied to an active TPS for a reentry vehicle. For those reasons, the concept of the electromagnetic flow control has been revisited in the reentry aerodynamic research field, and experimental [10, 11, 12] and numerical [13, 14, 15, 16, 17, 18] studies have been carried out in recent years.

Although these previous works have mostly clarified physical mechanisms of the electromagnetic flow control and approved its applicability to the reentry TPS in hypersonic continuum regimes, the flow control may be more suitable to aerocapture missions at more higher altitudes because the elctrodyanamic braking effect is more significant rather than its heat flux reduction effect [17, 18].

However the obtainable electrodynamic force is unknown in such a hypersonic rarefied regime. To investigate this topic, the present preliminary study simulates the electromagnetic flow control on a reentry Hayabusa-shape capsule entering a pure nitrogen atmosphere at the altitude of 80 km using the Direct Simulation Monte Carlo (DSMC) method [19] with a simple ion particle movement method like the Particle-In-Cell (PIC) method.

DSMC METHOD AND PHYSICAL MODEL

DSMC modeling

The present study simulates the flow field around the Hayabusa-shape capsule entering a pure nitrogen atmosphere, whose flow conditions are shown in Table 1. To simulate this hypersonic rarefied flow, we newly developed the axisymmetric DSMC code including chemical reactions with ionization and inelastic collisions among internal modes. The Ion-Averaged Velocity (IAV) method [20] is used to keep the charge-neutrality, in which electrons move at the ion velocity averaged in each cells. Ozawa et al. [21] recently have proposed the physical models for DSMC simulations in strongly thermochemical nonequilibrium conditions. The present study basically adopted their models to incorporate the thermochemical nonequilibrium effects, and more detailed description is found in [22].

Simple modeling of electromagnetic effect

The present study uses the IAV method, and hence ignores the detailed interaction between the electron movement and applied magnetic field; the Hall and ion slip effects and the resulting generation of the electric field are still not considered, although these effects are significant in rarefied ionized flows. [17, 18] Only interaction between an ion particle and the applied magnetic field are considered using the motion equation for the ion,

$$m_{\mathrm{ion}} d\boldsymbol{v}_{\mathrm{ion}}/dt = |e|\,\boldsymbol{v}_{\mathrm{ion}} \times \boldsymbol{B}(\boldsymbol{x}_{\mathrm{ion}}) \tag{2}$$

wherein $m_{\mathrm{ion}}, \boldsymbol{v}_{\mathrm{ion}}, \boldsymbol{x}_{\mathrm{ion}}, \boldsymbol{B}, |e|$ are respectively ion mass, the velocity and location of the ion particle, applied magnetic field at $\boldsymbol{x}_{\mathrm{ion}}$ and elementary charge. And this ion movement according to the electro-motive force $\boldsymbol{v}_{\mathrm{ion}} \times \boldsymbol{B}$ is solved using the leap-frog method like the PIC method.

Computational grid and applied field

Figure 2 shows the computational grid and applied magnetic field. The body shape is identical to that of the Hayabusa capsule forebody. The number of the cells are 200×120. The fine cells are prepared in the axial direction and the minimum size Δz is 0.1 mm which is the order of magnitude of the local mean free path.

Each cells are divided into 16 subcells to reduce the distance of the mean collision separation in selecting collisional pairs [19]. If the number of molecules in a cell is smaller than 20, the virtual subcell method [24] is used instead of searching a molecule-pair in subcells.

The magnetic filed $\boldsymbol{B}$ is applied on $r-z$ plane, in which a circular superconductive current loop embeded in the body is assumed to generate the magnetic filed of B_0=0.5−1 T at the stagnation point according to the Biot-Savart law.

RESULTS AND DISCUSSION

The present study sets the number of real particles represented by a macro-particle to be $N_0 = 5 \times 10^{12}$ in no radial weighting region ($r < r_{w,\mathrm{min}}$). The averaged number of macro-particles is 50-200 in any cell, but it is about 10 in the cells near the axis. This value might be too small to capture charged particles correctly whose molar fractions are smaller than 10%. The fluctuations of the solution near the axis are still large although the results are obtained after

approximately 30,000 sampling times (two days computations on a Core i7 personal computer). More sampling times and macro-particles or species weighting method [25] may be necessary to obtain more smooth results.

Ionizing flow without mangnetic field

Figures 3 and 4 show temperatures (heavy particle translational $T_{\rm trans}$, rotational $T_{\rm rot}$, vibrational $T_{\rm vib}$, and electron translational $T_{\rm e}$) and molar fractions on the ξ=3 line (ξ is grid number in the radial direction); the results on the axis are not shown beacuse the fluctuations of the solution are still large. Although the fluctuation of T_e is still large, the appearance of thermochimical noneqilibrium almost agrees with the resuls of the Stardust reentry [21, 23] whose flow conditions are very similar to those of this study.

The molar fraction of electron and σ are approximately 6% and 3,000 S/m (estimated using continuum cross sections of ionzied nitrogen gas[27, 28]) near the stagnation point. As a result, this flow should generate strong electrodyanmic force because Q parameter is estimated to be 5340($\gg 1$) if B=1 T.

Electromagnetic effect

Two cases of B_0=0.5 and 1 T are invesitaged. Figures 5 and 6 show the comparison of $T_{\rm trans}$ between applied and not-applied. The electro-motive force $\boldsymbol{v}_{{\rm ion},r,z}\times\boldsymbol{B}$ first acceleates ions in the θ direction, and then Lorentz force acting on the ion $\boldsymbol{F_L}$ is generated on $r-z$ plane by the electro-motive force $v_{{\rm ion},\theta}\boldsymbol{\theta}\times\boldsymbol{B}$. As a results, this strong F_L enlarges the shock layer in proportion to B^2, because Q parameter is proportional to B^2 if the detailed interactions (Hall and ion slip effects) between electrons and the magnetic field are ignored.

Figures 7, 8 and 9 show the comparison of $T_{\rm trans}$, $T_{\rm e}$, and the molar fraction of electron on ξ=3 line between applied and not-applied cases. The heat flux to the wall will reduce because $T_{\rm trans}$ near the wall decreases with increasing B, although the profile of B_0=0.5 T is questionable. The enlargement of the shock layer also enlarges the high T_e region and the resulting ionizing region (due to the avalanche ionization of No.4 in Table.2). As a results, the molar fraction of electron obtainable in B_0=1 T becomes four times as large as that of not-applied field.

Drag increment and heat flux reduction

The correct estimation of the electrodynamic drag is difficult because of ignoring the real electron motion due to the useage of the IAV method in this study; Hence F_L exerted on ions is simply doubled on the assumption that electrons receive the Lorentz force identical to that of ions. Axial electrodynamic drag exerted on the superconductive coil are defined as

$$D_L = -2\int_{\rm all\,cells}\sum_{ions} F_{L,z}dV \tag{3}$$

Figures 10 and 11 show D_L, aerodynamic drag D_A, and heat flux to the body wall. In contrast to the drastic increase of D_L, D_A decreases with B because of the deviation of the flow from the body. Eventually, the total drag increase is 5% in applying B=1 T. However, this result is questionable because the shock layer enlargement is very large. More discussions will be necessary to estimate the electrodynamic drag correctly. As was expected, the heat flux decreases with B, and 15% reduction is achievable in B=1 T.

SUMMARY

To investigate the electrodynamic aerobraking in a hypersonic rarefied regime, the electromagnetic flow control on a reentry Hayabusa-shape capsule entering a pure nitrogen atmosphere is investigated using the Direct Simulation Monte Carlo method with a simple ion particle movement method like the Particle-In-Cell method. As a results, the generated electrodynamic force is found to be enough strong to use the electrodynamic aerobraking in the hypersonic rarefied regime: 5% increase of the total drag and 15% reduction of the heat flux are achievable in applying B=1 T. However, more correct treatment of the electron motion (e.g., DSMC/PIC/electron-fluid Hybrid method [29, 30]) will be necessary to estimate the electrodynamic drag force correctly, and we will try this method in the future work.

TABLE 1. Flow conditions

Gas	Pure nitrogen
Altitude h	80 km
Flight velocity v_∞	12.3 km/s
Number density n_∞	$3.97\times10^{20}\,\mathrm{m}^{-3}$
Temperature T_∞	199 K
Body diameter D	40.4 cm
Knudsen number K_{n_∞} (based on D)	1.75×10^{-2}

TABLE 2. Chemical reactions [21]

No.	Reaction		
1a	N_2+M	$\Rightarrow$	$N+N+M$
1b*	N_2+A	$\Rightarrow$	$N+N+A$
1c	N_2+e	$\Rightarrow$	$N+N+e$
2	$N+N$	$\Leftrightarrow$	$N_2^+ +e$
3	N_2+N^+	$\Leftrightarrow$	$N+N_2^+$
4	$N+e$	$\Rightarrow$	$N^+ +e+e$

M: any third body molecule
A: any third body atom,* [23]

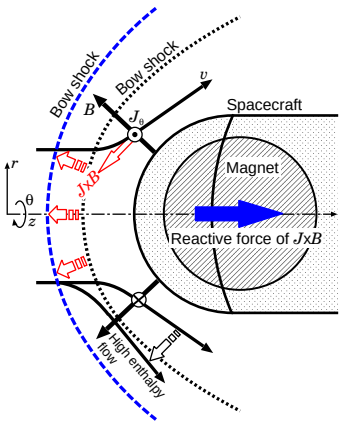

FIGURE 1. Schematic view of the electrodynamic aerobraking.

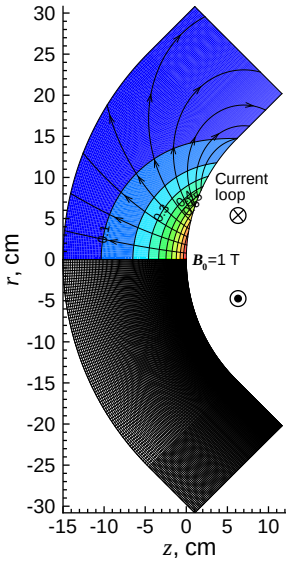

FIGURE 2. Computational grids and applied filed.

ACKNOWLEDGMENTS

This research was supported by the Grant-in-Aids for Young Scientists (B) (No. 22760624, 2010) from the Japan Society for the Promotion of Science.

REFERENCES

1. Smith, J. C., and Bell J. L., "2001 Mars Odyssey Aerobraking", *Journal of Spacecraft and Rockets*, Vol. 42, No. 3, pp. 406–415.
2. Rohrschneider, R. R., and Braun, R. D., "Survey of Ballute Technology for Aerocapture," *Journal of Spacecraft and Rockets*, Vol. 44, No. 1, pp. 10–23.
3. Kantrowitz, A. R., "A Survey of Physical Phenomena Occurring in Flight at Extreme Speeds," *Proceedings of the Conference on High-Speed Aeronautics*, edited by Ferri, A., Hoff, N. J., and Libby P. A., Polytechnic Institute of Brooklyn, New York, 1955, pp. 335–339.
4. Resler, E. L., and Sears, W. R., "The Prospects of Magnetoaerodynamics," *Journal of Aeronautical Science*, Vol. 25, 1958, pp. 235–245.
5. Ericson, W. B., and Maciulaitis, A., "Investigation of Magnetohydrodynamic Flight Control," *Journal of Spacecraft and Rockets*, Vol. 1, No. 3, 1964, pp. 283–289.
6. Sutton, G. W., and Sherman A., "Engineering Magnetohydrodynamics," Dover, New York, 1965.
7. Ziemer, R. W., and Bush, W. B. "Magnetic Field Effects on Bow Shock Stand-Off Distance," *Physical Review Letters*, Vol. 1, No. 2, 1958, pp. 58–59.
8. Nowak, R. J., and Yuen, M. C., "Heat Transfer to a Hemispherical Body in a Supersonic Argon Plasma," *AIAA Journal*, Vol. 11, No. 11, 1973, pp. 1463–1464.

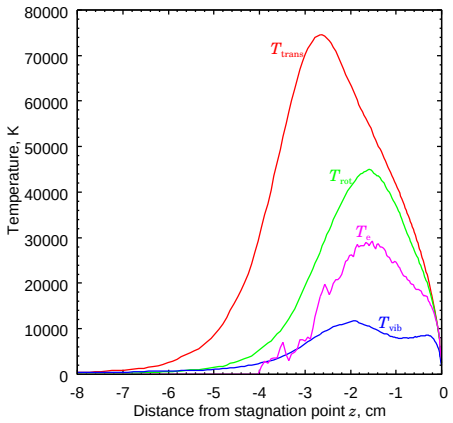

FIGURE 3. Temperature on ξ=3 line in ionizing flow

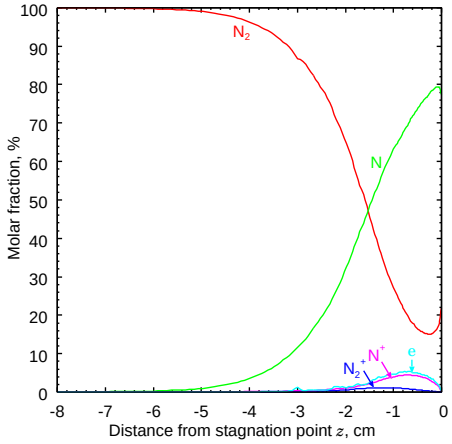

FIGURE 4. Molar fractions on ξ=3 line in ionizing flow

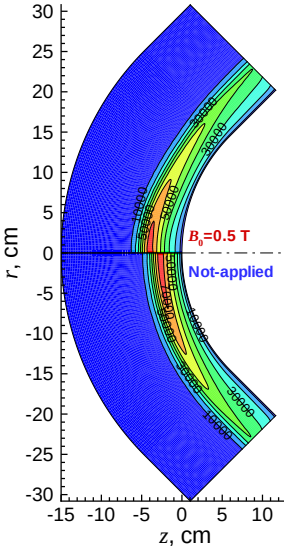

FIGURE 5. T_{trans} [K] contours (B_0=0.5 T)

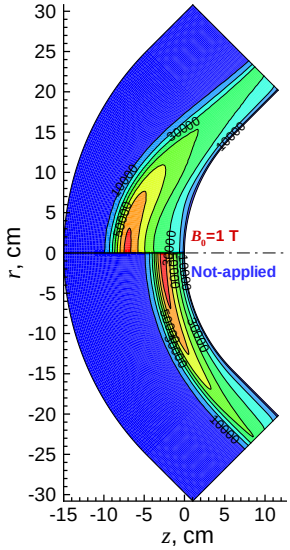

FIGURE 6. T_{trans} [K] contours (B_0=1 T)

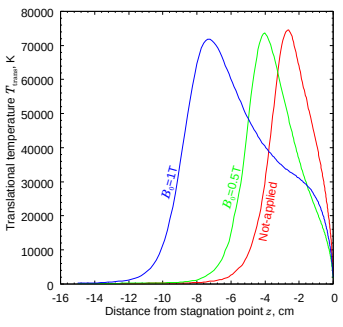

FIGURE 7. T_{trans} on ξ=3 line in not- and applied cases

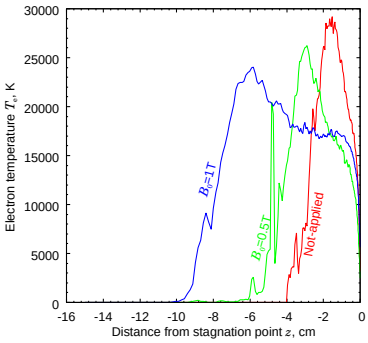

FIGURE 8. T_{e} on ξ=3 line in not- and applied cases

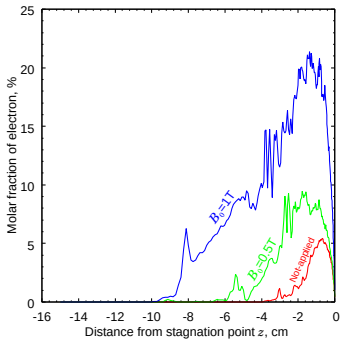

FIGURE 9. Molar fraction of electron on ξ=3 line in not- and applied cases

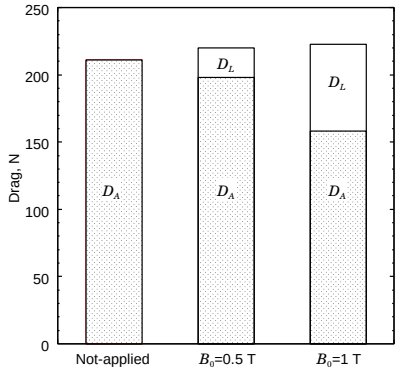

FIGURE 10. Drag force

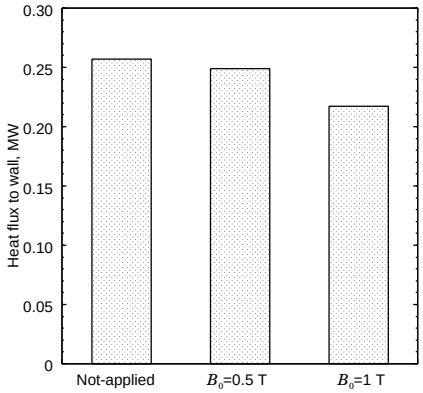

FIGURE 11. Heat flux to wall

9. Nowak, R, J., Kranc, S., Porter, R. W., Yuen, M. C., and Cambel, A. B., "Magnetogasdynamic Re-Entry Phenomena," *Journal of Spacecraft and Rockets*, Vol. 4, No. 11, 1967, pp. 1538–1542.
10. Takizawa, Y., Matsuda, A., Sato, S., Abe, T., and Konigorski, D., "Experimental Investigation of the Electromagnetic Effect on a Shock Layer around a Blunt Body in a Weakly Ionized Flow," *Physics of Fluids*, Vol. 18, No. 11, 117105, 2006.
11. Matsuda, A., Wakatsuki, K., Takizawa, Y., Kawamura, M., Otsu, H., Konigorski, D., Sato, S., and Abe, T., "Shock Layer Enhancement by Electro-Magnetic Effect for a Spherically Blunt Body", AIAA Paper 2006-3573, 2006.
12. Kawamura, M., Matsuda, A., Katsurayama, H., Otsu, H., Konigorski, D., and Abe, T., "Experiment on Drag Enhancement for a Blunt Body with Electrodynamic Heat Shield," *Journal of Spacecraft and Rockets*, Vol. 46, No. 6, pp.1171-1177, 2009.
13. Poggie, J., and Gaitonde, V., "Magnetic Control of Flow past a Blunt Body: Numerical Validation and Exploration," *Physics of Fluids*, Vol. 14, No. 5, 2002, pp. 1720–1731.
14. Otsu, H., Abe, T., and Konigorski, D., "Influence of the Hall Effect on the Electrodynamic Heat Shield System for Reentry Vehicles," AIAA Paper 2005-5049, 2005.
15. Fujino, T., Sugita, H., Mizuno, M., Funaki, I., and Ishikawa, M., "Influences of Electrical Conductivity of Wall on Magnetohydrodynamic Control of Aerodynamic Heating," *Journal of Spacecraft and Rockets*, Vol. 43, No. 1, 2006, pp. 63–70.
16. Katsurayama, H., Kawamura, M., Matsuda, A., and Abe, T., "Particle Simulation of Electromagnetic Control of a Weakly Ionized Flow past a Blunt Body," AIAA Paper 2007-1439.
17. Katsurayama, H., Kawamura, M., Matsuda, A., and Abe, T., "Numerical Study of the Electromagnetic Control of a Weakly Ionized Flow around a Blunt Body: Role of a Insulative Boundary in the Flow," AIAA Paper 2007-4529.
18. Katsurayama, H., and Abe, T., "Numerical Simulation of Electromagnetic Flow Control in a One-Kilowatt Class Argon Arcjet Windtunnel," AIAA Paper 2008-4016, 2008.
19. Bird, G. A., "Molecular Gas Dynamics and the Direct Simulation of Gas Flows," Oxford University Press, New York, 1994.
20. Boyd, I. D., "Monte Carlo Simulation of Nonequilibrium Flow in a Low-Power Hydrogen Arcjet," *Physics of Fluid*, Vol. 9, No. 10, pp.3086-3095, 1997.
21. Ozawa, T., Zhong, J., and Levin, D. A., "Development of Kinetic-Based Energy Exchange Models for Noncontinuum, Ionized Hypersonic Flows," *Physics of Fluids*, Vol. 20, 046102, 2008.
22. Katsurayama, H., and Abe, T., "Particle Simulation of Electrodynamic Aerobraking on a Reentry Capsule," AIAA Paper 2010-4491.
23. Boyd, I. D., Trumble, K., and Wright, M. J., "Nonequilibrium Particle and Continuum Analyses of Stardust Entry for Near-Continuum Conditions," AIAA Paper 2007-4543, 2007.
24. LeBeau, G. J. and Boyles, K. A., "Virtual Sub-Cells for the Direct Simulation Monte Carlo Method," AIAA Paper 2003-1031, 2003.
25. Boyd, I. D, "Conservative Species Weighting Scheme for the Direct Simulation Monte Carlo Method," *Journal of Thermophysics and Heat Transfer*, Vol. 10, No. 4, pp.579-585, 1996.
26. Farbar, E. D. and Boyd, I. D., "Simulation of FIRE II Reentry Flow Using the Direct Simulation Monte Carlo Method," AIAA 2008-4103.
27. Capitelli, M., Gorse, C., and Longo, S., "Collision Integrals of High-Temperature Air Species," *Journal of Thermophysics and Heat Transfer*, Vol. 14, No. 2, pp.259-268, 2000.
28. Wright, M. J., Bose, D., Palmer, G. E., Levin, E., "Recommended Collision Integrals for Transport Property Computations, Part I: Air Species," *AIAA Journal* Vol. 43, No. 12, pp.2558-2564, 2005.
29. Gatsonis, N. A., and Yin X., "Hybrid (Particle-Fluid) Modeling of Pulsed Plasma Thruster Plumes," *Journal of Propulsion and Power*, Vol. 17, No. 5, 2001, pp. 945–957.
30. Choi, Y., Boyd, I. D., and Keidar, M., "Effect of a Magnetic Field in Simulating the Plume Field of an Anode Layer Hall Thruster," *Journal of Applied Physics*, Vol. 105, 013303, 2009.